



Nonlinear modeling and dynamic analysis of bioengineering hyper-elastic tubes based on different material models

Seyed Sajad Mirjavadi¹ · Masoud Forsat¹ · Salman Badnava²

Received: 18 August 2019 / Accepted: 14 November 2019 / Published online: 17 December 2019
© Springer-Verlag GmbH Germany, part of Springer Nature 2019

Abstract

In this research, nonlinear vibrations of a hyper-elastic tube accounting for large deflection and moderate rotation have been examined. The hyper-elastic tube is assumed to be surrounded by a nonlinear hardening elastic medium. Different types of hyper-elastic material models are presented and discussed including neo-Hookean, Mooney–Rivlin, Ishihara and Yeoh models. The efficacy of these models in nonlinear vibration modeling and analysis of hyper-elastic tubes has been examined. Modified von-Karman strain is used to consider both large deflection and moderate rotation. The governing equations are obtained based on strain energy function of above-mentioned hyper-elastic material models. The nonlinear governing equation of the tube contains cubic and quantic terms which is solved via extended Hamiltonian method leading to a closed form of nonlinear vibration frequency. The effect of hyper-elastic models and their material parameters on nonlinear vibrational frequency of tubes has been studied.

Keywords Bioengineering material · Nonlinear vibration · Hyper-elastic material · Yeoh model · Moderate rotation · Hamiltonian method

1 Introduction

Silicone rubber is classified in the category of hyper-elastic materials and possesses excellent biomedical compatibility and chemical resistance together with complex mechanical properties. Hyper-elastic materials undergo large strains under various loading conditions. Hence, their mechanical characteristics cannot be described using a linear stress–strain relationship (Shahzad et al. 2015). Therefore, hyper-elastic materials exhibit material nonlinearity and there is a need for nonlinear stress–strain relations to express their constitutive laws. Up to now, several models are proposed for modeling of hyper-elastic materials such as neo-Hookean, Mooney–Rivlin, Ishihara, Ogden and Yeoh models (Martins et al. 2006; Ogden et al. 2004; Horgan and Saccomandi 2006). These models require material

parameters to define the stress–strain relation. The simplest approach to obtain these material parameters is performing uniaxial or biaxial tension tests (Marckmann and Verron 2006; Beda 2007). Then, the constitutive hyper-elastic material models can be fitted to the test data based on specified values of material parameters.

Structures made of hyper-elastic materials exhibit large deformation during their operational life. When investigating vibration behavior of hyper-elastic structures, it is important to consider large strain effects. Based on von-Karman's strain model, many investigations consider large deflections in analysis of nonlinear structures (Li and Hu 2016; Barati and Shahverdi 2018a; Shahverdi et al. 2019; Besseghier et al. 2015; Bouiadjra et al. 2013; She et al. 2018a). In this model, only large deflection of the structures has been considered and rotations are considered to be small (Barati and Zenkour 2019; Sheng and Wang 2018; She et al. 2018b). This assumption is mostly used for elastic structures. When the rotations are not small enough, the modified von-Karman nonlinear strain is used to account for both large deflection and moderately large rotation of the structure (Reddy and El-Borgi 2014; Reddy and Srinivasa 2014).

Many investigations are published on nonlinear vibrations of hyper-elastic structures. Breslavsky et al. (2014) studied nonlinear vibration behavior of thin hyper-elastic

✉ Seyed Sajad Mirjavadi
seyedsajadmjirjavadi@gmail.com
Masoud Forsat
masoudforsatlar@gmail.com

¹ Department of Mechanical and Industrial Engineering, Qatar University, P.O. Box 2713, Doha, Qatar

² Department of Electrical Engineering, Qatar University, Doha, Qatar

plates made of rubber and soft biological tissues. They used neo-Hookean, Mooney–Rivlin and Ogden hyper-elastic laws to examine nonlinear vibration of the plate. Soares and Gonçalves (2018) examined nonlinear vibration of hyper-elastic plates rested on elastic foundations by considering pre-stretch effect. Wang et al. (2019) studied vibration behavior of axially moving beams made of hyper-elastic material accounting for large deformations. Also, Barforooshi and Mohammadi (2016) and Mohammadi and Barforooshi (2017) used hyper-elastic material laws to examine nonlinear vibrations of beam-type resonators. They used von-Karman strain type in order to capture large deflections of the beam under oscillation.

This paper is concerned with the study of nonlinear vibrational behavior of hyper-elastic tubes accounting for large deflection and moderate rotation. Hyper-elastic tubes have many applications especially at bioengineering and mechanical engineering fields. The hyper-elastic tube is assumed to be surrounded by a nonlinear hardening elastic medium. Various types of hyper-elastic material models have been introduced including neo-Hookean, Mooney–Rivlin, Ishihara and Yeoh models. Large deflections and also moderately large rotation of the tube have been considered based on modified von-Karman strain model. Nonlinear vibration frequency of the tube is obtained by solving the tube governing equation based on extended Hamiltonian approach. The effects of hyper-elastic material parameters, hyper-elastic material law, nonlinear elastic medium, length-to-thickness ratio and boundary condition on vibrational frequency of hyper-elastic tube have been studied in detail.

2 Different models for hyper-elastic materials

Based on the approach of developing strain energy function (W), there are three types of models for hyper-elastic materials (Marckmann and Verron 2006; Steinmann et al. 2012):

1. Phenomenological models: they are based on the mathematical development of strain energy function, for example Rivlin series.
2. Models based on direct determination of material parameters using experiment.
3. Physically based models: they consider the physical properties of polymeric chains network and statistical approaches to develop strain energy function.

In the following, some well-known models of hyper-elastic materials will be introduced and discussed. The strain energy function based on these models is based on strain invariants (I_1, I_2, I_3) which are (Steinmann et al. 2012; Ali et al. 2010):

$$\begin{aligned} I_1 &= \lambda_1^2 + \lambda_2^2 + \lambda_3^2 = \text{tr}(C) \\ I_2 &= \lambda_1^2 \lambda_2^2 + \lambda_1^2 \lambda_3^2 + \lambda_2^2 \lambda_3^2 = \frac{1}{2}(I_1^2 - \text{tr}(C^2)) \\ I_3 &= \lambda_1^2 \lambda_2^2 \lambda_3^2 = \det(C) \end{aligned} \quad (1)$$

where λ_i ($i = 1, 2, 3$) denote the square roots for right Cauchy–Green strains tensor (C) and physically they are stretch ratios. Also, based on incompressibility assumption of materials, $I_3 = 1$. Also, the right Cauchy–Green strains tensor (C) is corresponding to strains tensor of the beam (E) as:

$$[C] = 2[E] + [I]. \quad (2)$$

2.1 Neo-Hookean type

The neo-Hookean type has only one material constant (C_1) and is known as simplest model for hyper-elastic materials. It is a physically based model and introduces the strain energy function as follows:

$$W = c_{10}(I_1 - 3) \quad (3)$$

where I_1 is the first strain invariant. For a rubber material, it is found that $C_{10} = 0.2$ MPa. In literature, it is reported that such modeling does not have enough terms for mathematical description of beams or plates to obtain their governing equations. So, this model has been discarded in the present paper due to its limitations.

2.2 Mooney–Rivlin model

As reported by Mooney, the response of rubber subjected to simple shear is linear. Based on two material parameters (C_{10} and C_{01}), the strain energy function based on this model can be expressed as:

$$W = c_{10}(I_1 - 3) + c_{01}(I_2 - 3) \quad (4)$$

where I_1 and I_2 , respectively, denote the first and second strain invariants. This model is suitable for moderate deformations, lower than 200% and is erroneous for larger deformations. Similar to neo-Hookean model, Mooney–Rivlin model has not adequate terms to include nonlinear strains of the beam. So, the governing equations will not completely be derived. So, there is a need for another complete model of hyper-elastic materials.

2.3 Yeoh type

This type only depends on the first strain invariant (I_1) and is phenomenological type, but introduces three material parameters (c_{10}, c_{20}, c_{30}). The strain energy function based on this model can be expressed as:

$$W = c_{10}(I_1 - 3) + c_{20}(I_1 - 3)^2 + c_{30}(I_1 - 3)^3. \tag{5}$$

This model is successfully used by many researchers. The efficacy of this model in modeling of hyper-elastic material structures will be figured out in the following sections. For silicone rubber, the parameters are reported as (Martins et al. 2006): $c_{10} = 0.24162$ MPa, $c_{20} = 0.19977$ MPa, and $c_{30} = -0.00541$ MPa.

2.4 Three-parameter Mooney–Rivlin model

This modeling is an extension of Mooney–Rivlin type with two parameters, and it is also called Ishihara model. Hence, this model contains three material parameters and the strain energy function has the following form:

$$W = c_{10}(I_1 - 3) + c_{01}(I_2 - 3) + c_{20}(I_1 - 3)^2. \tag{6}$$

3 Mathematical formulation

For modeling of hyper-elastic tube shown in Fig. 1, the well-known Euler–Bernoulli beam model has been utilized for which the displacement field ($u_1, u_2=0, u_3$) can be introduced as follows by neglecting shear deformation impacts (Bouadi et al. 2018; Bourada et al. 2018; Younsi et al. 2018; Mokhtar et al. 2018; Boutaleb et al. 2019; Abdelaziz et al. 2017; Faleh et al. 2018a, b; Al-Maliki et al. 2019; Fenjan et al. 2019; Ahmed et al. 2019):

Herein, W defines strain energy function, V defines work done by external forces, and K defines kinetic energy.

Based on Yeoh or three-parameter Mooney–Rivlin models, the first strain energy variation might be generally defined as:

$$\delta W = \delta W_{10} + \delta W_{01} + \delta W_{20} + \delta W_{30} \tag{11}$$

where using Eqs. (5) and (6) one can get to:

$$\delta W_{10} = 4C_{10} \int \frac{\partial w}{\partial x} \delta \left(\frac{\partial w}{\partial x} \right) dV = 4AC_{10} \frac{\partial w}{\partial x} \delta w \Big|_{x=0}^{x=L} - 4AC_{10} \int_0^L \frac{\partial^2 w}{\partial x^2} \delta(w) dx \tag{12}$$

$$\begin{aligned} \delta W_{01} = & 4C_{01} \int \left(2 \frac{\partial w}{\partial x} \delta \left(\frac{\partial w}{\partial x} \right) + \frac{1}{2} \left(\frac{\partial w}{\partial x} \right)^2 \delta \left(\frac{\partial u}{\partial x} \right) + \frac{\partial u}{\partial x} \frac{\partial w}{\partial x} \delta \left(\frac{\partial w}{\partial x} \right) + \left(\frac{\partial w}{\partial x} \right)^3 \delta \left(\frac{\partial w}{\partial x} \right) \right) dV \\ = & 8AC_{01} \frac{\partial w}{\partial x} \delta w \Big|_{x=0}^{x=L} - 8AC_{01} \int_0^L \frac{\partial^2 w}{\partial x^2} \delta(w) dx + 2AC_{01} \left(\frac{\partial w}{\partial x} \right)^2 \delta u \Big|_{x=0}^{x=L} - 4AC_{01} \int_0^L \frac{\partial w}{\partial x} \frac{\partial^2 w}{\partial x^2} \delta(u) dx \\ & + 4AC_{01} \frac{\partial u}{\partial x} \frac{\partial w}{\partial x} \delta w \Big|_{x=0}^{x=L} - 4AC_{01} \int_0^L \left(\frac{\partial u}{\partial x} \frac{\partial^2 w}{\partial x^2} + \frac{\partial w}{\partial x} \frac{\partial^2 u}{\partial x^2} \right) \delta(w) dx + 4AC_{01} \left(\frac{\partial w}{\partial x} \right)^3 \delta w \Big|_{x=0}^{x=L} \\ & - 12AC_{01} \int_0^L \left(\frac{\partial w}{\partial x} \right)^2 \frac{\partial^2 w}{\partial x^2} \delta(w) dx \end{aligned} \tag{13}$$

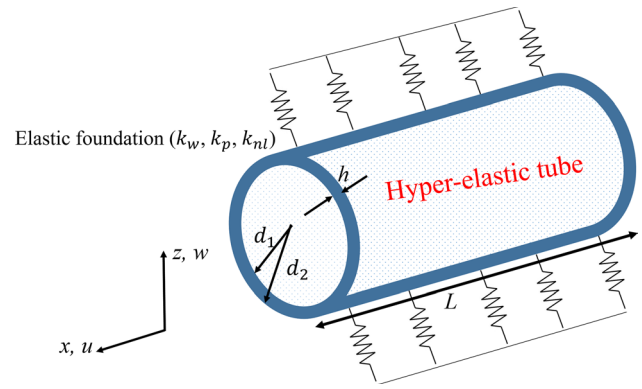


Fig. 1 Configuration of hyper-elastic tube embedded in elastic medium

$$u_1(x, y, z, t) = u(x, y, t) - z \frac{\partial w}{\partial x} \tag{7}$$

$$u_3(x, y, z, t) = w(x, y, t) \tag{8}$$

Here, u and w , respectively, introduce longitudinal and lateral displacements. Based on modified von-Karman’s nonlinearity, the strain field in axial and transverse directions may be defined as (Reddy and Srinivasa 2014):

$$\begin{aligned} \epsilon_{xx} &= \frac{\partial u_1}{\partial x} = \frac{\partial u}{\partial x} - z \frac{\partial^2 w}{\partial x^2} + \frac{1}{2} \left(\frac{\partial w}{\partial x} \right)^2 \\ \epsilon_{zz} &= \frac{1}{2} \theta_x^2, \theta_x = -\frac{\partial w}{\partial x} \end{aligned} \tag{9}$$

where the transverse strain (ϵ_{zz}) is created due to moderate rotation (θ_x^2). To derive the governing equations of hyper-elastic tube, the extended Hamilton’s principle may be defined as:

$$\int_0^t \delta(W + V - K) dt = 0. \tag{10}$$

$$\begin{aligned}
\delta W_{20} &= 4C_{20} \int \left(2 \frac{\partial u}{\partial x} \delta \left(\frac{\partial u}{\partial x} \right) + 2 \left(\frac{\partial w}{\partial x} \right)^2 \delta \left(\frac{\partial u}{\partial x} \right) + 4 \frac{\partial u}{\partial x} \frac{\partial w}{\partial x} \delta \left(\frac{\partial w}{\partial x} \right) + 2z^2 \frac{\partial^2 w}{\partial x^2} \delta \left(\frac{\partial^2 w}{\partial x^2} \right) + 4 \left(\frac{\partial w}{\partial x} \right)^3 \delta \left(\frac{\partial w}{\partial x} \right) \right) dV \\
&= 8C_{20}A \frac{\partial u}{\partial x} \delta u \Big|_{x=0}^{x=L} - 8C_{20}A \int_0^L \frac{\partial^2 u}{\partial x^2} \delta(u) dx + 8C_{20}A \left(\frac{\partial w}{\partial x} \right)^2 \delta u \Big|_{x=0}^{x=L} - 16AC_{20} \int_0^L \frac{\partial^2 w}{\partial x^2} \frac{\partial w}{\partial x} \delta(u) dx \\
&\quad + 16C_{20}A \frac{\partial u}{\partial x} \frac{\partial w}{\partial x} \delta w \Big|_{x=0}^{x=L} - 16AC_{20} \int_0^L \left(\frac{\partial^2 w}{\partial x^2} \frac{\partial u}{\partial x} + \frac{\partial^2 u}{\partial x^2} \frac{\partial w}{\partial x} \right) \delta(w) dx + 8C_{20}I \frac{\partial^2 w}{\partial x^2} \delta \left(\frac{\partial w}{\partial x} \right) \Big|_{x=0}^{x=L} \\
&\quad - 8C_{20}I \frac{\partial^3 w}{\partial x^3} \delta(w) \Big|_{x=0}^{x=L} + 8C_{20}I \int_0^L \frac{\partial^4 w}{\partial x^4} \delta(w) dx \\
&\quad + 16AC_{20} \left(\frac{\partial w}{\partial x} \right)^3 \delta(w) \Big|_{x=0}^{x=L} - 48C_{20}A \int_0^L \frac{\partial^2 w}{\partial x^2} \left(\frac{\partial w}{\partial x} \right)^2 \delta(w) dx
\end{aligned} \tag{14}$$

$$\begin{aligned}
\delta W_{10} &= 8C_{30} \int \left(3 \left(\frac{\partial u}{\partial x} \right)^2 \delta \left(\frac{\partial u}{\partial x} \right) + 6 \frac{\partial u}{\partial x} \left(\frac{\partial w}{\partial x} \right)^2 \delta \left(\frac{\partial u}{\partial x} \right) + 6 \frac{\partial w}{\partial x} \left(\frac{\partial u}{\partial x} \right)^2 \delta \left(\frac{\partial w}{\partial x} \right) + 3z^2 \left(\frac{\partial^2 w}{\partial x^2} \right)^2 \delta \left(\frac{\partial u}{\partial x} \right) \right. \\
&\quad + 6z^2 \frac{\partial u}{\partial x} \frac{\partial^2 w}{\partial x^2} \delta \left(\frac{\partial^2 w}{\partial x^2} \right) + 3 \left(\frac{\partial w}{\partial x} \right)^4 \delta \left(\frac{\partial u}{\partial x} \right) + 12 \frac{\partial u}{\partial x} \left(\frac{\partial w}{\partial x} \right)^3 \delta \left(\frac{\partial w}{\partial x} \right) + 6z^2 \frac{\partial^2 w}{\partial x^2} \left(\frac{\partial w}{\partial x} \right)^2 \delta \left(\frac{\partial^2 w}{\partial x^2} \right) \\
&\quad \left. + 6z^2 \left(\frac{\partial^2 w}{\partial x^2} \right)^2 \frac{\partial w}{\partial x} \delta \left(\frac{\partial w}{\partial x} \right) + 6 \left(\frac{\partial w}{\partial x} \right)^5 \delta \left(\frac{\partial w}{\partial x} \right) \right) dV \\
&= 24C_{30}A \left(\frac{\partial u}{\partial x} \right)^2 \delta u \Big|_{x=0}^{x=L} - 48C_{30}A \int_0^L \frac{\partial u}{\partial x} \frac{\partial^2 u}{\partial x^2} \delta(u) dx + 48C_{30}A \frac{\partial u}{\partial x} \left(\frac{\partial w}{\partial x} \right)^2 \delta u \Big|_{x=0}^{x=L} \\
&\quad - 48C_{30}A \int_0^L \left(\frac{\partial^2 u}{\partial x^2} \left(\frac{\partial w}{\partial x} \right)^2 + 2 \frac{\partial u}{\partial x} \frac{\partial w}{\partial x} \frac{\partial^2 w}{\partial x^2} \right) \delta(u) dx + 48C_{30}A \frac{\partial w}{\partial x} \left(\frac{\partial u}{\partial x} \right)^2 \delta w \Big|_{x=0}^{x=L} \\
&\quad - 48C_{30}A \int_0^L \left(\frac{\partial^2 w}{\partial x^2} \left(\frac{\partial u}{\partial x} \right)^2 + 2 \frac{\partial u}{\partial x} \frac{\partial w}{\partial x} \frac{\partial^2 u}{\partial x^2} \right) \delta(w) dx + 24C_{30}I \left(\frac{\partial^2 w}{\partial x^2} \right)^2 \delta u \Big|_{x=0}^{x=L} \\
&\quad - 48C_{30}I \int_0^L \frac{\partial^3 w}{\partial x^3} \frac{\partial^2 w}{\partial x^2} \delta(u) dx + 48C_{30}I \frac{\partial u}{\partial x} \frac{\partial^2 w}{\partial x^2} \delta \left(\frac{\partial w}{\partial x} \right) \Big|_{x=0}^{x=L} - 48C_{30}I \left(\frac{\partial^2 u}{\partial x^2} \frac{\partial^2 w}{\partial x^2} + \frac{\partial u}{\partial x} \frac{\partial^3 w}{\partial x^3} \right) \delta w \Big|_{x=0}^{x=L} \\
&\quad + 48C_{30}A \int_0^L \left(\frac{\partial^2 w}{\partial x^2} \frac{\partial^3 u}{\partial x^3} + 2 \frac{\partial^3 w}{\partial x^3} \frac{\partial^2 u}{\partial x^2} + \frac{\partial u}{\partial x} \frac{\partial^4 w}{\partial x^4} \right) \delta(w) dx + 24C_{30}A \left(\frac{\partial w}{\partial x} \right)^4 \delta u \Big|_{x=0}^{x=L} \\
&\quad - 96C_{30}A \int_0^L \left(\frac{\partial w}{\partial x} \right)^3 \frac{\partial^2 w}{\partial x^2} \delta(u) dx + 96C_{30}A \left(\frac{\partial w}{\partial x} \right)^3 \frac{\partial u}{\partial x} \delta w \Big|_{x=0}^{x=L} \\
&\quad - 96C_{30}A \int_0^L \left(3 \frac{\partial^2 w}{\partial x^2} \left(\frac{\partial w}{\partial x} \right)^2 \frac{\partial u}{\partial x} + \left(\frac{\partial w}{\partial x} \right)^3 \frac{\partial^2 u}{\partial x^2} \right) \delta(w) dx \\
&\quad + 48C_{30}I \left(\frac{\partial w}{\partial x} \right)^2 \frac{\partial^2 w}{\partial x^2} \delta \left(\frac{\partial w}{\partial x} \right) \Big|_{x=0}^{x=L} \\
&\quad - 48C_{30}I \left(\left(\frac{\partial w}{\partial x} \right)^2 \frac{\partial^3 w}{\partial x^3} + 2 \frac{\partial w}{\partial x} \left(\frac{\partial^2 w}{\partial x^2} \right)^2 \right) \delta(w) \Big|_{x=0}^{x=L} \\
&\quad + 48C_{30}I \int_0^L \left(\frac{\partial^4 w}{\partial x^4} \left(\frac{\partial w}{\partial x} \right)^2 + 6 \frac{\partial^3 w}{\partial x^3} \frac{\partial^2 w}{\partial x^2} \frac{\partial w}{\partial x} + 2 \left(\frac{\partial^2 w}{\partial x^2} \right)^3 \right) \delta(w) dx \\
&\quad + 48C_{30}I \left(\frac{\partial^2 w}{\partial x^2} \right)^2 \frac{\partial w}{\partial x} \delta w \Big|_{x=0}^{x=L} - 48C_{30}I \int_0^L \left(2 \frac{\partial^3 w}{\partial x^3} \frac{\partial^2 w}{\partial x^2} \frac{\partial w}{\partial x} + \left(\frac{\partial^2 w}{\partial x^2} \right)^3 \right) \delta(w) dx \\
&\quad + 48C_{30}A \left(\frac{\partial w}{\partial x} \right)^5 \delta w \Big|_{x=0}^{x=L} - 240C_{30}A \int_0^L \left(\frac{\partial w}{\partial x} \right)^4 \frac{\partial^2 w}{\partial x^2} \delta(w) dx.
\end{aligned} \tag{15}$$

The first variation applied to external load work may be written as follows:

$$\delta V = \int_0^L q \delta w dx. \tag{16}$$

$$q = k_w w - k_p \frac{\partial^2 w}{\partial x^2} + k_{nl} w^3 \tag{17}$$

where k_w and k_p are Winkler and Pasternak coefficients of the substrate, respectively. Next, k_{nl} denotes the nonlinear stiffness of the surrounding medium. The variation of kinetic energy is represented by:

$$\delta K = \int_0^L \left(I_0 \left[\frac{\partial u}{\partial t} \frac{\partial \delta u}{\partial t} + \left(\frac{\partial w}{\partial t} \right) \left(\frac{\partial \delta w}{\partial t} \right) \right] - I_1 \left(\frac{\partial u}{\partial t} \frac{\partial^2 \delta w}{\partial x \partial t} + \frac{\partial^2 w}{\partial x \partial t} \frac{\partial \delta u}{\partial t} \right) + I_2 \left(\frac{\partial^2 w}{\partial x \partial t} \frac{\partial^2 \delta w}{\partial x \partial t} \right) \right) dx \tag{18}$$

Applied load by the substrate should be defined as (Bakhadda et al. 2018; Yazid et al. 2018; Kadari et al. 2018; Chaabane et al. 2019; Boukhlif et al. 2019; Boulefrakh et al. 2019):

where

$$(I_0, I_1, I_2) = \int_{-h/2}^{h/2} (1, z, z^2) \rho dz. \tag{19}$$

The nonlinear governing equations may be derived for hyper-elastic tube by using Eqs. (12)–(18) as:

$$\begin{aligned} & -4AC_{01} \frac{\partial w}{\partial x} \frac{\partial^2 w}{\partial x^2} - 8C_{20}A \frac{\partial^2 u}{\partial x^2} - 16AC_{20} \frac{\partial^2 w}{\partial x^2} \frac{\partial w}{\partial x} - 48C_{30}A \frac{\partial u}{\partial x} \frac{\partial^2 u}{\partial x^2} \\ & - 48C_{30}A \left(\frac{\partial^2 u}{\partial x^2} \left(\frac{\partial w}{\partial x} \right)^2 + 2 \frac{\partial u}{\partial x} \frac{\partial w}{\partial x} \frac{\partial^2 w}{\partial x^2} \right) - 48C_{30}I \frac{\partial^3 w}{\partial x^3} \frac{\partial^2 w}{\partial x^2} - 96C_{30}A \left(\frac{\partial w}{\partial x} \right)^3 \frac{\partial^2 w}{\partial x^2} \\ & = I_0 \frac{\partial^2 u}{\partial t^2} - I_1 \frac{\partial^3 w}{\partial x \partial t^2} \end{aligned} \tag{20}$$

$$\begin{aligned} & -4AC_{10} \frac{\partial^2 w}{\partial x^2} - 8AC_{01} \frac{\partial^2 w}{\partial x^2} - 4AC_{01} \left(\frac{\partial u}{\partial x} \frac{\partial^2 w}{\partial x^2} + \frac{\partial w}{\partial x} \frac{\partial^2 u}{\partial x^2} \right) \\ & - 12AC_{01} \left(\frac{\partial w}{\partial x} \right)^2 \frac{\partial^2 w}{\partial x^2} - 16AC_{20} \left(\frac{\partial^2 w}{\partial x^2} \frac{\partial u}{\partial x} + \frac{\partial^2 u}{\partial x^2} \frac{\partial w}{\partial x} \right) + 8C_{20}I \frac{\partial^4 w}{\partial x^4} \\ & - 48C_{20}A \frac{\partial^2 w}{\partial x^2} \left(\frac{\partial w}{\partial x} \right)^2 - 48C_{30}A \left(\frac{\partial^2 w}{\partial x^2} \left(\frac{\partial u}{\partial x} \right)^2 + 2 \frac{\partial u}{\partial x} \frac{\partial w}{\partial x} \frac{\partial^2 u}{\partial x^2} \right) \\ & + 48C_{30}A \left(\frac{\partial^2 w}{\partial x^2} \frac{\partial^3 u}{\partial x^3} + 2 \frac{\partial^3 w}{\partial x^3} \frac{\partial^2 u}{\partial x^2} + \frac{\partial u}{\partial x} \frac{\partial^4 w}{\partial x^4} \right) - 96C_{30}A \left(3 \frac{\partial^2 w}{\partial x^2} \left(\frac{\partial w}{\partial x} \right)^2 \frac{\partial u}{\partial x} + \left(\frac{\partial w}{\partial x} \right)^3 \frac{\partial^2 u}{\partial x^2} \right) \\ & + 48C_{30}I \left(\frac{\partial^4 w}{\partial x^4} \left(\frac{\partial w}{\partial x} \right)^2 + 6 \frac{\partial^3 w}{\partial x^3} \frac{\partial^2 w}{\partial x^2} \frac{\partial w}{\partial x} + 2 \left(\frac{\partial^2 w}{\partial x^2} \right)^3 \right) - 48C_{30}I \left(2 \frac{\partial^3 w}{\partial x^3} \frac{\partial^2 w}{\partial x^2} \frac{\partial w}{\partial x} + \left(\frac{\partial^2 w}{\partial x^2} \right)^3 \right) \\ & - 240C_{30}A \left(\frac{\partial w}{\partial x} \right)^4 \frac{\partial^2 w}{\partial x^2} = I_0 \frac{\partial^2 u}{\partial t^2} - I_1 \frac{\partial^3 w}{\partial x \partial t^2} \\ & = +I_0 \frac{\partial^2 w}{\partial t^2} + I_1 \left(\frac{\partial^3 u}{\partial x \partial t^2} \right) - I_2 \nabla^2 \left(\frac{\partial^2 w}{\partial t^2} \right) - k_w w + k_p \nabla^2 w - k_{nl} w^3. \end{aligned} \tag{21}$$

Note that $I_1 = 0$ for isotropic hyper-elastic material.

4 Solution procedure

In this section, nonlinear vibration problem of hyper-elastic tubes is solved using a Hamiltonian approach and with the help of Galerkin’s method. First, it should be mentioned that the effect of axial displacement is ignorable compared to transverse displacement (She et al. 2018a). However, the transverse displacement is assumed to be:

$$w = \sum_{i=1}^{\infty} W_i \varphi_i(x) \tag{22}$$

where W_i is the vibration amplitude. The boundary conditions based on transverse displacement from Eqs. (12)–(15) can be expressed as:

$$w|_{x=0} = w|_{x=L} = 0, \quad \frac{\partial^2 w}{\partial x^2} \Big|_{x=0} = \frac{\partial^2 w}{\partial x^2} \Big|_{x=L} = 0$$

Simply - Supported (S – S) (23)

$$w|_{x=0} = w|_{x=L} = 0, \quad \frac{\partial w}{\partial x} \Big|_{x=0} = \frac{\partial w}{\partial x} \Big|_{x=L} = 0$$

Clamped - Clamped (C – C). (24)

To satisfy above-mentioned boundary condition, the function $\varphi_i(x)$ may be selected as (Bourada et al. 2018; Younsi et al. 2018; Mokhtar et al. 2018):

$$\varphi_i(x) = \sin\left(\frac{i\pi}{L}x\right) \quad \text{for S – S} \tag{25}$$

$$\varphi_i(x) = 0.5\left(1 - \cos\left(\frac{2i\pi}{L}x\right)\right) \quad \text{for C – C} \tag{26}$$

Now, placing Eq. (22) into the governing Eq. (21) and using Galerkin’s method lead to the following simplified nonlinear equation:

$$K_1 W + K_3 W^3 + K_5 W^5 + M \ddot{W} = 0. \tag{27}$$

The symbol (.) represents the derivative with respect to time, M is mass matrix, and K_i are structural stiffness:

$$\begin{aligned} K_1 &= -4A(C_{10} + 2C_{01})Z_{20} + 8C_{20}IZ_{40} + k_w Z_{00} - k_p Z_{20} \\ K_3 &= -12AC_{01}Z_{2110} - 48C_{20}AZ_{2110} \\ &\quad + 48C_{30}I(Z_{4110} + 4Z_{3210} + Z_{2220}) + k_{nl}Z_{0000} \\ K_5 &= -240C_{30}AZ_{211110} \\ M &= I_0 Z_{00} - I_2 Z_{20}. \end{aligned} \tag{28}$$

In above equation, the constructed integrals are:

$$\begin{aligned} Z_{00} &= \int_0^L \varphi_i \varphi_i dx \\ Z_{20} &= \int_0^L \varphi_i'' \varphi_i dx \\ Z_{40} &= \int_0^L \varphi_i'''' \varphi_i dx \\ Z_{11} &= \int_0^L \varphi_i' \varphi_i' dx \\ Z_{0000} &= \int_0^L (\varphi_i)^4 dx \\ Z_{2110} &= \int_0^L \varphi_i'' \varphi_i' \varphi_i' dx \\ Z_{2220} &= \int_0^L \varphi_i'' \varphi_i'' \varphi_i'' dx \\ Z_{3210} &= \int_0^L \varphi_i''' \varphi_i'' \varphi_i' dx \\ Z_{4110} &= \int_0^L \varphi_i'''' \varphi_i' \varphi_i' dx \\ Z_{211110} &= \int_0^L \varphi_i'' (\varphi_i')^4 dx. \end{aligned} \tag{29}$$

In above integrals, the symbol prime defines the derivatives with respect to x .

4.1 Extended Hamiltonian method

The nonlinear governing equation of hyper-elastic tube, Eq. (27), contains cubic and quantic terms. Hamiltonian approach (He 2010) is mostly used for Duffing-type oscillator having only cubic nonlinearity. In order to solve Eq. (27), an extended version of Hamiltonian method is used in the present research (Bayat et al. 2014).

Hamiltonian of a conservative system will be constant during vibrations. Hence, the Hamiltonian of the governing equation of the tube can be expressed as:

$$\begin{aligned} H &= +\frac{1}{2}M\dot{W}^2 + \frac{1}{2}K_1 W^2 + K_3\left(\frac{1}{4}\tilde{W}^4\right) + K_5\left(\frac{1}{6}\tilde{W}^6\right) \\ &= \text{Constant} = H_0. \end{aligned} \tag{30}$$

Above relation gives that $H - H_0 = 0$. Therefore, from mathematical point of view, it can be concluded that (Barati 2018a, b; Barati and Shahverdi 2018b):

$$\frac{\partial H}{\partial W} = 0. \tag{31}$$

For this approach, the following function should be defined as:

$$\tilde{H}(t) = \int_0^{T/4} H dt = \frac{1}{4} TH. \tag{32}$$

Note that T defines the vibrations period and from above relation one can conclude that:

$$\frac{\partial \tilde{H}(t)}{\partial T} = \frac{1}{4} H. \tag{33}$$

According to Eqs. (31) and (33), it may be deduced that

$$\frac{\partial}{\partial \tilde{W}} \left(\frac{\partial \tilde{H}(t)}{\partial T} \right) = 0. \tag{34}$$

The presented Eq. (34) can be also represented as:

$$\frac{\partial}{\partial \tilde{W}} \left(\frac{\partial \tilde{H}(t)}{\partial (1/\omega_{NL})} \right) = 0. \tag{35}$$

For nonlinear harmonic oscillation of the tube, the vibration amplitude can be defined as (Barati 2018a, b; Barati and Shahverdi 2018b):

$$W(t) = \tilde{W} \cos(\omega t) \tag{36}$$

Now, with the use of Eq. (36), one can express Eq. (32) in detailed form as:

$$\begin{aligned} \tilde{H}(\omega_{NL}) = \frac{1}{\omega_{NL}} \int_0^{\pi/2} \left[+ \left(\frac{1}{2} M \tilde{W}^2 \right) \omega_{NL}^2 \sin^2(\theta) + \left(\frac{1}{2} K_1 \tilde{W}^2 \right) \cos^2(\theta) + K_3 \left(\frac{1}{4} \tilde{W}^4 \right) \cos^4(\theta) \right. \\ \left. + K_5 \left(\frac{1}{6} \tilde{W}^6 \right) \cos^6(\theta) \right] d\theta. \end{aligned} \tag{37}$$

The stationary conditions $\partial \tilde{H} / \partial \tilde{W} = 0$ result in

$$\frac{K_1}{M} \tilde{W} + \frac{3}{4} \frac{K_3}{M} (\tilde{W})^3 + \frac{5}{8} \frac{K_5}{M} (\tilde{W})^5 - \omega^2 \tilde{W} = 0. \tag{38}$$

Finally, the nonlinear frequency of hyper-elastic tube is derived as:

$$\omega_{NL} = \frac{1}{2} \sqrt{\frac{8 \frac{K_1}{M} + 6 \frac{K_3}{M} (\tilde{W})^2 + 5 \frac{K_5}{M} (\tilde{W})^4}{2}}. \tag{39}$$

In the present article, results are presented based on the following normalized quantities:

$$\Omega = \omega_{NL} L \sqrt{\frac{\rho}{c_{10}}}, \quad K_w = k_w \frac{L^4}{c_{10} d_2^4}, \quad K_p = k_p \frac{L^2}{c_{10} d_2^4}, \quad K_{NL} = k_{nl} \frac{L^4}{c_{10} h}. \tag{40}$$

5 Discussions on results

In present section, geometrically nonlinear vibrations characteristics of hyper-elastic tubes have been studied and figured out. Two types of hyper-elastic material models, called three-parameter Mooney–Rivlin model (Ishihara model) and Yeoh model, are considered. In previous section, closed form of nonlinear vibration frequency of the tube was obtained. The effects of hyper-elastic material parameters, hyper-elastic material law, nonlinear elastic medium, length-to-thickness ratio and boundary conditions on vibration frequency of the hyper-elastic tube will be studied in detail.

Vibration frequency validation of a hyper-elastic beam with rectangular cross section based on Yeoh model is presented in Fig. 2 with those of Barforooshi and Mohammadi (2016), and a good agreement has been achieved among the curves. The thickness of hyper-elastic beam is considered as $h=0.65$. For this validation, the effect moderate rotations has been discarded due to the reason that in the paper of Barforooshi and Mohammadi (2016), and moderate rotations are not considered. However, the geometric nonlinearity in this figure is considered based on large deflection of the hyper-elastic beam.

Nonlinear vibration frequency versus dimensionless amplitude of hyper-elastic tube based on Yeoh and three-

parameter Mooney–Rivlin hyper-elastic models is plotted in Fig. 3 when $L/h=20$. Both S–S and C–C boundary conditions have been considered. First of all, it must be pointed out that increasing of vibrational amplitudes is corresponding to greater frequency owing to inclusion of nonlinear stiffening impacts. However, the smallest frequency of the tube can be obtained at $\tilde{W}/h=0$. Also, as the value of vibration amplitude increases, the difference between vibration frequencies of these two models becomes greater. This is due to the difference of these models in incorporation of strains for modeling of hyper-elastic materials. Also, consideration of mechanism of deformation has some differences for these models. Yeoh model contains the nonlinear strain up to third order, but three-parameter Mooney–Rivlin contains the strain up to second order. In fact, Yeoh model captures larger strains than Mooney–Rivlin in modeling of hyper-elastic materials.

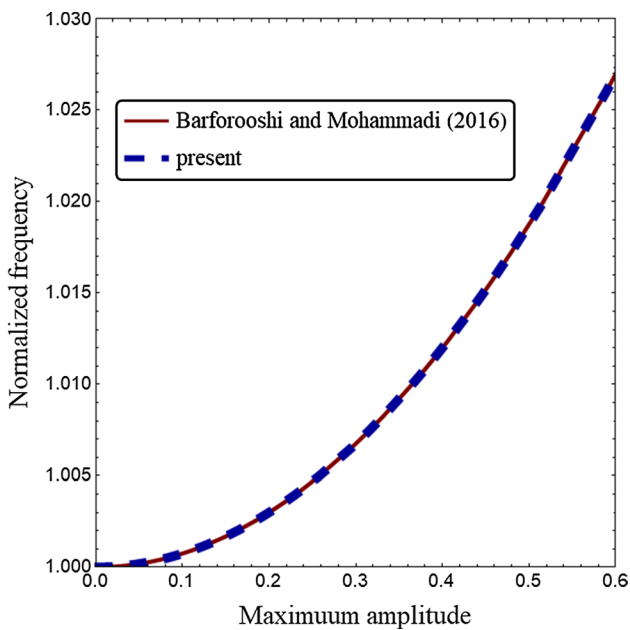


Fig. 2 Validation of the nonlinear vibration frequency for a hyper-elastic beam

As it is well known on the literature, obtaining hyper-elastic material parameter is a complex task since they are dependent on various conditions such as loading type and environment. When using optimization to obtain material

models, it is important to note that the answer is an approximation within predefined tolerances of the correct one. In Fig. 4, the effect of hyper-elastic material parameters of Yeoh model (c_{10} , c_{20} , c_{30}) with $\pm 10\%$ and $\pm 20\%$ tolerance is presented. One can see that increase in c_{10} parameter reduces the nonlinear vibration frequency, but increase in c_{20} parameter increases the nonlinear vibration frequency. This is due to the fact that increase in c_{20} parameter increases structural stiffness of the tube. Also, c_{30} is a material parameter related to larger strains, as can be seen from Eq. (5). Thus, from Fig. 4, it is obvious that the effect of c_{30} material parameter is not sensible at small vibration amplitudes.

Effect of slenderness ratio (L/h) on nonlinear vibration behavior of hyper-elastic tubes with S–S and C–C boundary conditions is presented in Fig. 5. Yeoh model of hyper-elastic materials is considered in this figure. It is known that tubes become more flexible at greater values for slenderness ratio. Thus, derived nonlinear vibration frequencies become lower by increasing of slenderness ratios at constant normalized amplitudes (\bar{W}/h). Moreover, derived nonlinear vibration frequencies related to several values for slenderness ratios rely on values of non-dimensional amplitudes. At a small slenderness ratio, nonlinear vibration frequency increases with higher slope with respect to non-dimensional amplitudes than a large slenderness ratio.

Figures 6 and 7 show the dependency of nonlinear free vibration characteristics of geometrically nonlinear

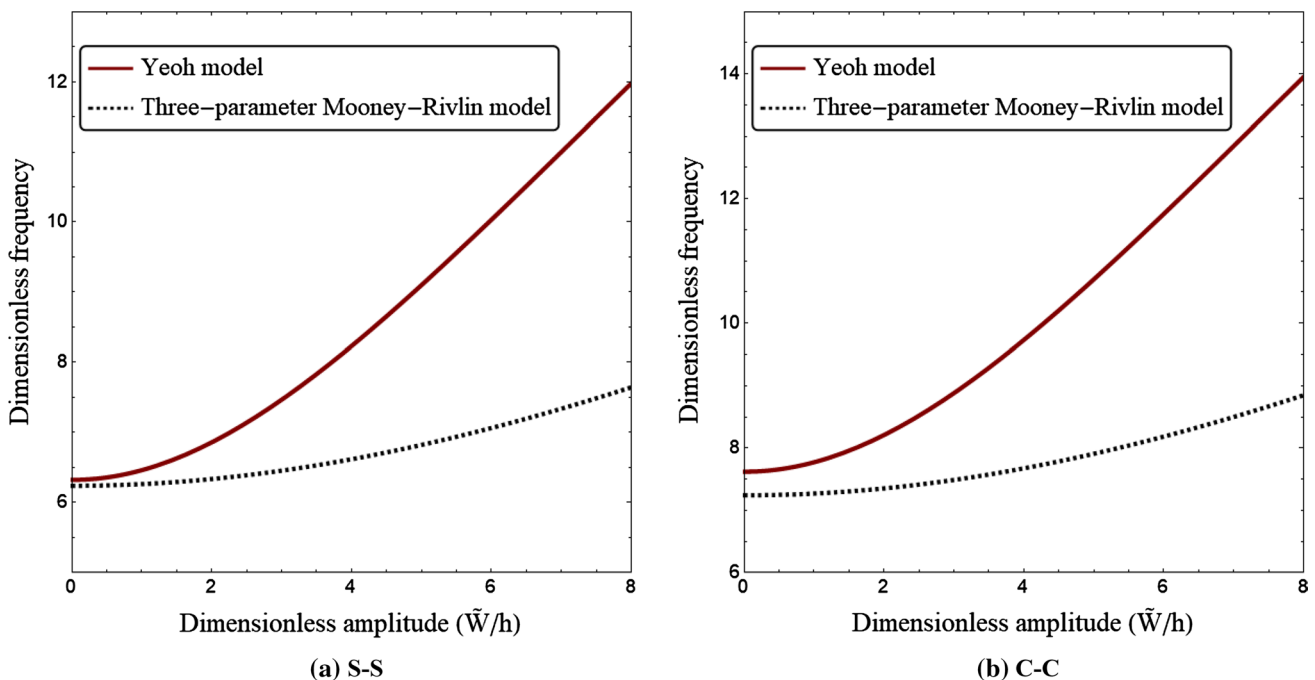


Fig. 3 Nonlinear vibrational frequency versus dimensionless amplitude based on various hyper-elastic models ($L/h=20$)

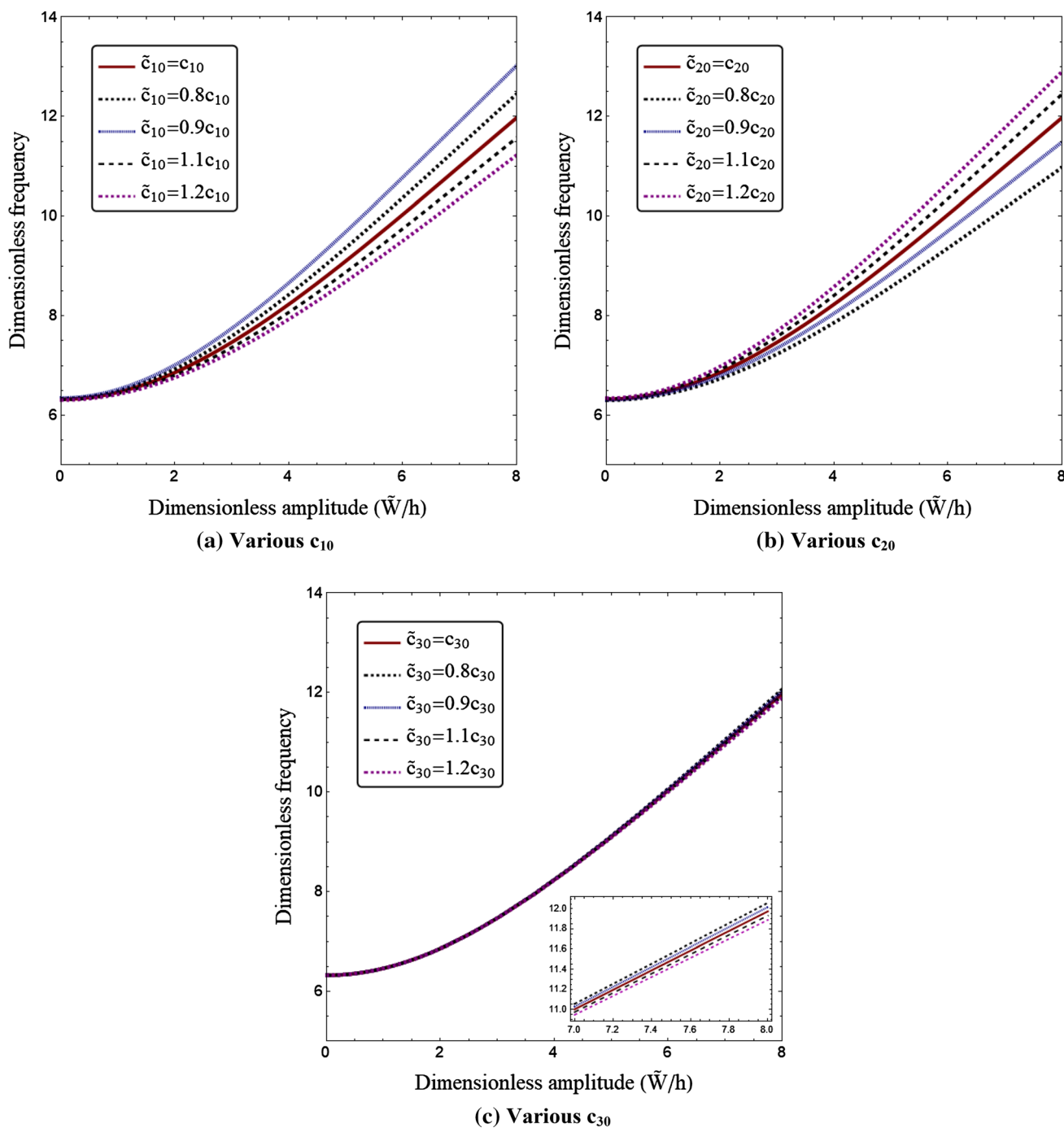


Fig. 4 Nonlinear vibrational frequency versus dimensionless amplitude based on various hyper-elastic material parameters ($L/h = 20$)

hyper-elastic tubes on elastic medium parameters. It is clear from the figure that increase in Winkler (K_w) and Pasternak (K_p) elastic medium coefficients only increases the value of vibration frequency and their influences are not dependent on the vibrational amplitudes. In fact, nonlinear vibration frequency is increased with the increase in elastic medium parameters regardless of the magnitude of

vibration amplitude. In can be concluded that this observation is related to the increase in bending rigidity of the tube by considering the influence of elastic medium.

The effect of nonlinear parameter of elastic medium (K_{NL}) on vibration frequency of hyper-elastic tubes is depicted in Fig. 8 when $K_w = 100$, $K_p = 10$. It is obvious based on the figure that the influences of nonlinear elastic medium

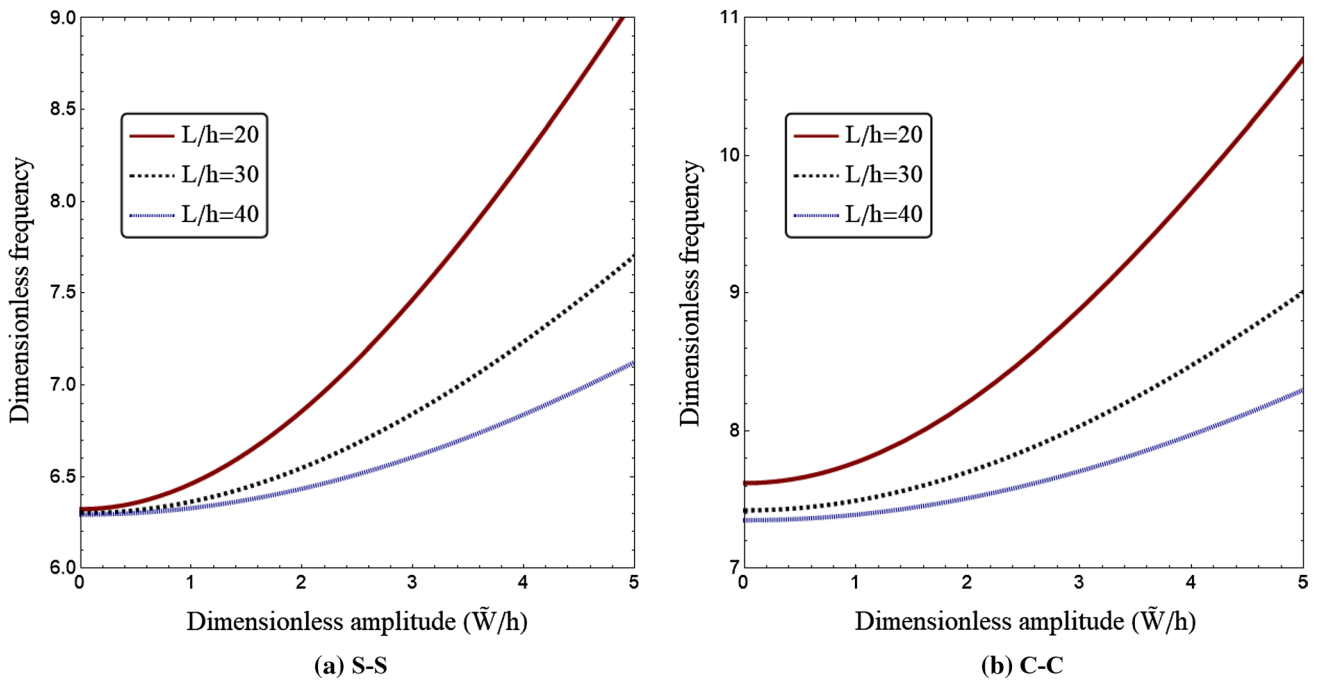


Fig. 5 Nonlinear vibration frequency versus dimensionless amplitude based on various slenderness ratios

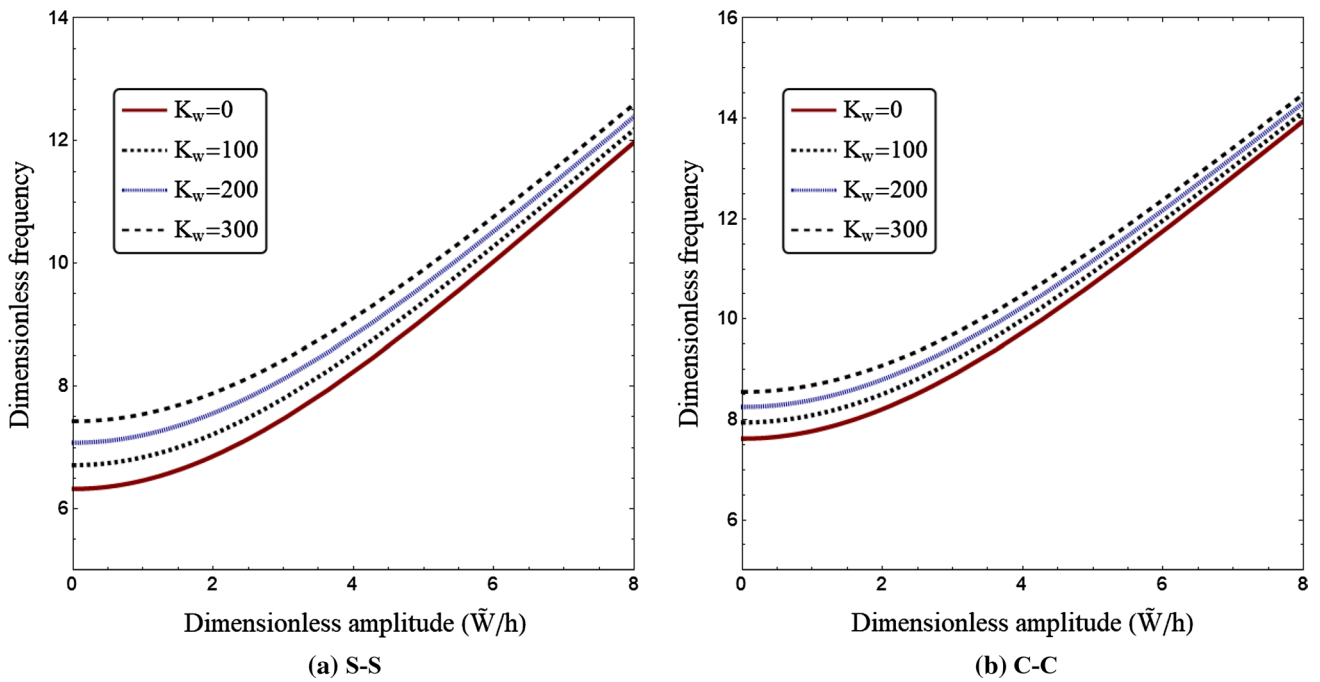


Fig. 6 Nonlinear vibration frequency versus dimensionless amplitude based on various Winkler parameters ($L/h = 50, K_p = 0$)

constant (K_{NL}) on vibrational frequencies are negligible near the zero vibrational amplitudes. Hence, its impacts become more announced at great vibrational amplitudes. Actually,

nonlinear elastic medium coefficient cannot vary the value of natural frequency, the frequency at $\tilde{W}/h = 0$, because the natural frequency is independent of nonlinear stiffness. However, as the magnitudes of vibration amplitudes become

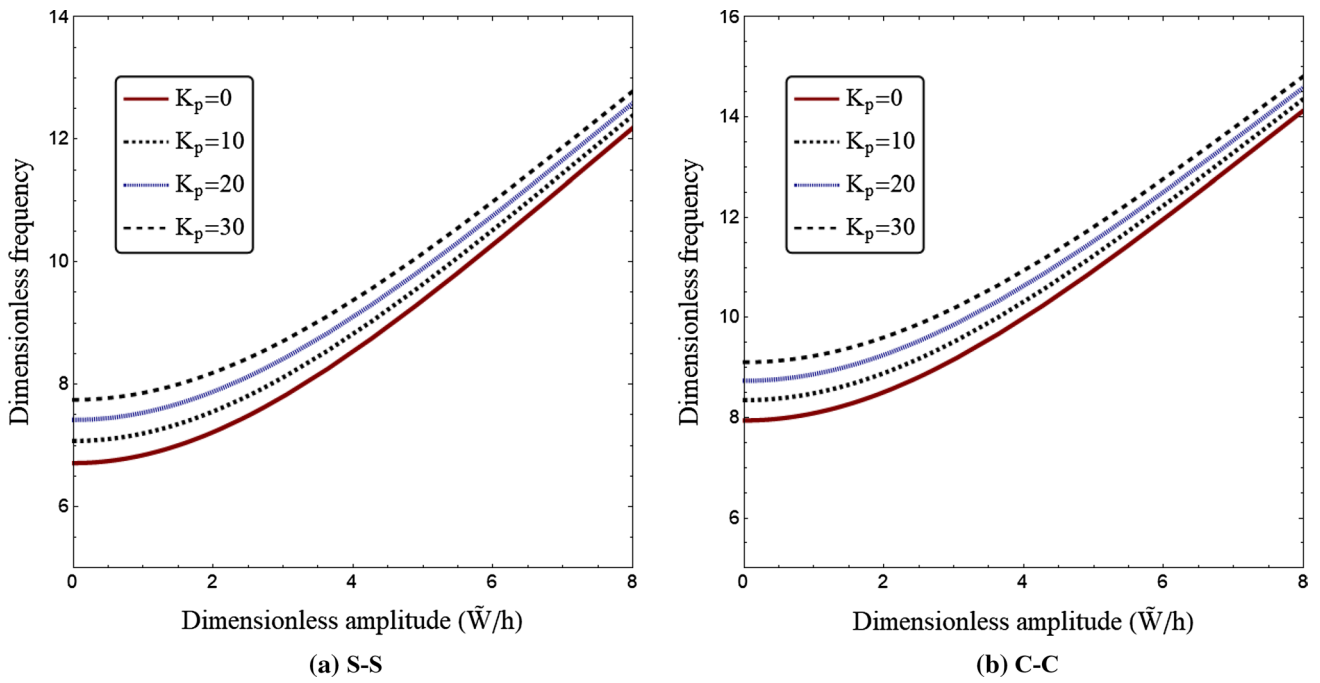


Fig. 7 Nonlinear vibration frequency versus dimensionless amplitude based on various Pasternak parameters ($L/h = 50, K_w = 100$)

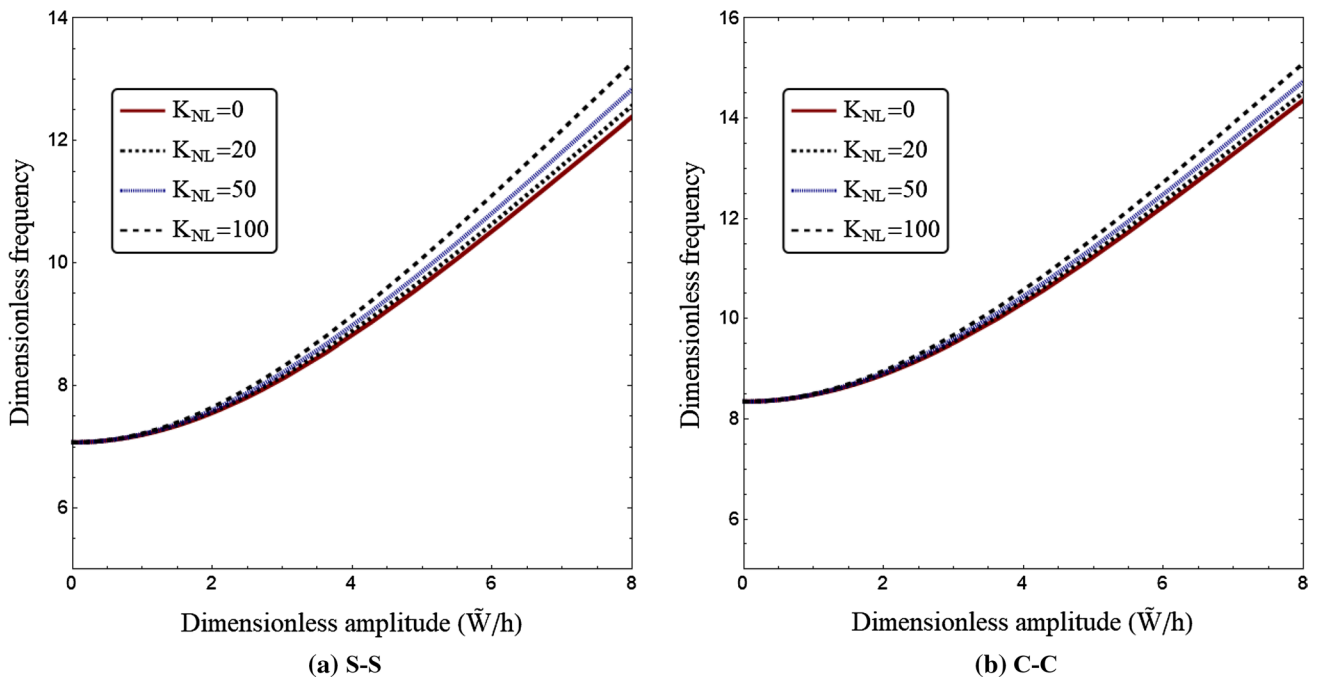


Fig. 8 Nonlinear vibration frequency versus dimensionless amplitude based on various nonlinear elastic medium parameters ($L/h = 20, K_w = 100, K_p = 10$)

higher, the influence of nonlinear elastic medium parameter on the vibration frequency becomes more prominent because of the enhancement of nonlinear hardening influences.

6 Conclusions

The present paper dealt with nonlinear vibration analysis of a hyper-elastic tube made of silicone rubber which is

embedded in a nonlinear elastic medium. Yeoh and three-parameter Mooney–Rivlin models were used for modeling of hyper-elastic material. Extended Hamiltonian approach was used for solving the nonlinear governing equation of the tube possessing cubic and quintic nonlinearity types. It was found that as the value of vibration amplitude increased, the difference between vibration frequencies of Yeoh and three-parameter Mooney–Rivlin models became greater. This is due to the difference of these models in incorporation of strains for modeling of hyper-elastic materials. Also, it was reported that increase in c_{10} and c_{20} parameters, respectively, reduced and increased the nonlinear vibration frequency. Also, the effect of c_{30} material parameter was not sensible at small vibration amplitudes.

Acknowledgements The authors would like to thank Fidar Project Qaem (FPQ) for providing the fruitful and useful help.

Compliance with ethical standards

Conflict of interest The authors declare that they have no conflict of interest.

References

- Abdelaziz et al (2017) An efficient hyperbolic shear deformation theory for bending, buckling and free vibration of FGM sandwich plates with various boundary conditions. *Steel Compos Struct* 25(6):693–704
- Ahmed RA, Fenjan RM, Faleh NM (2019) Analyzing post-buckling behavior of continuously graded FG nanobeams with geometrical imperfections. *Geomech Eng* 17(2):175–180
- Ali A, Hosseini M, Sahari BB (2010) A review and comparison on some rubber elasticity models. *J Sci Ind Res* 69(7):495–500
- Al-Maliki AF, Faleh NM, Alasadi AA (2019) Finite element formulation and vibration of nonlocal refined metal foam beams with symmetric and non-symmetric porosities. *Struct Monit Maint* 6(2):147–159
- Bakhadda et al (2018) Dynamic and bending analysis of carbon nanotube-reinforced composite plates with elastic foundation. *Wind Struct* 27(5):311–324
- Barati MR (2018a) Investigating nonlinear vibration of closed circuit flexoelectric nanobeams with surface effects via Hamiltonian method. *Microsyst Technol* 24(4):1841–1851
- Barati MR (2018b) Closed-form nonlinear frequency of flexoelectric nanobeams with surface and nonlocal effects under closed circuit electric field. *Mater Res Exp* 5(2):025008
- Barati MR, Shahverdi H (2018a) Nonlinear vibration of nonlocal four-variable graded plates with porosities implementing homotopy perturbation and Hamiltonian methods. *Acta Mech* 229(1):343–362
- Barati MR, Shahverdi H (2018b) Nonlinear thermal vibration analysis of refined shear deformable FG nanoplates: two semi-analytical solutions. *J Braz Soc Mech Sci Eng* 40(2):64
- Barati MR, Zenkour AM (2019) Analysis of postbuckling of graded porous GPL-reinforced beams with geometrical imperfection. *Mech Adv Mater Struct* 26(6):503–511
- Barforooshi SD, Mohammadi AK (2016) Study neo-Hookean and Yeoh hyper-elastic models in dielectric elastomer-based micro-beam resonators. *Latin Am J Solids Struct* 13(10):1823–1837
- Bayat M, Pakar I, Cveticanin L (2014) Nonlinear vibration of stringer shell by means of extended Hamiltonian approach. *Arch Appl Mech* 84(1):43–50
- Beda T (2007) Modeling hyperelastic behavior of rubber: a novel invariant-based and a review of constitutive models. *J Polym Sci B Polym Phys* 45(13):1713–1732
- Besseghier A, Heireche H, Bousahla AA, Tounsi A, Benzair A (2015) Nonlinear vibration properties of a zigzag single-walled carbon nanotube embedded in a polymer matrix. *Adv Nano Res* 3(1):029
- Bouadi et al (2018) A new nonlocal HSDT for analysis of stability of single layer graphene sheet. *Adv Nano Res* 6(2):147–162
- Bouiadjra RB, Bedia EA, Tounsi A (2013) Nonlinear thermal buckling behavior of functionally graded plates using an efficient sinusoidal shear deformation theory. *Struct Eng Mech* 48(4):547–567
- Boukhelif et al (2019) A simple quasi-3D HSDT for the dynamics analysis of FG thick plate on elastic foundation. *Steel Compos Struct* 31(5):503–516
- Boulefrakh et al (2019) The effect of parameters of visco-Pasternak foundation on the bending and vibration properties of a thick FG plate. *Geomech Eng* 18(2):161–178
- Bourada et al (2018) A novel refined plate theory for stability analysis of hybrid and symmetric S-FGM plates. *Struct Eng Mech* 68(6):661–675
- Boutaleb et al (2019) Dynamic analysis of nanosize FG rectangular plates based on simple nonlocal quasi 3D HSDT. *Adv Nano Res* 7(3):189–206
- Breslavsky ID, Amabili M, Legrand M (2014) Nonlinear vibrations of thin hyperelastic plates. *J Sound Vib* 333(19):4668–4681
- Chaabane et al (2019) Analytical study of bending and free vibration responses of functionally graded beams resting on elastic foundation. *Struct Eng Mech* 71(2):185–196
- Faleh NM, Ahmed RA, Fenjan RM (2018a) On vibrations of porous FG nanoshells. *Int J Eng Sci* 133:1–14
- Faleh NM, Fenjan RM, Ahmed RA (2018b) Dynamic analysis of graded small-scale shells with porosity distributions under transverse dynamic loads. *Eur Phys J Plus* 133(9):348
- Fenjan RM, Ahmed RA, Alasadi AA, Faleh NM (2019) Nonlocal strain gradient thermal vibration analysis of double-coupled metal foam plate system with uniform and non-uniform porosities. *Coupled Syst Mech* 8(3):247–257
- He JH (2010) Hamiltonian approach to nonlinear oscillators. *Phys Lett A* 374(23):2312–2314
- Horgan CO, Saccomandi G (2006) Phenomenological hyperelastic strain-stiffening constitutive models for rubber. *Rubber Chem Technol* 79(1):152–169
- Kadari et al (2018) Buckling analysis of orthotropic nanoscale plates resting on elastic foundations. *J Nano Res* 55:42–56
- Li L, Hu Y (2016) Nonlinear bending and free vibration analyses of nonlocal strain gradient beams made of functionally graded material. *Int J Eng Sci* 107:77–97
- Marckmann G, Verron E (2006) Comparison of hyperelastic models for rubber-like materials. *Rubber Chem Technol* 79(5):835–858
- Martins PALS, Natal Jorge RM, Ferreira AJM (2006) A comparative study of several material models for prediction of hyperelastic properties: application to silicone-rubber and soft tissues. *Strain* 42(3):135–147
- Mohammadi AK, Barforooshi SD (2017) Nonlinear forced vibration analysis of dielectric-elastomer based micro-beam with considering Yeoh hyper-elastic model. *Latin Am J Solids Struct* 14(4):643–656
- Mokhtar et al (2018) A novel shear deformation theory for buckling analysis of single layer graphene sheet based on nonlocal elasticity theory. *Smart Struct Syst* 21(4):397–405

- Ogden RW, Saccomandi G, Sgura I (2004) Fitting hyperelastic models to experimental data. *Comput Mech* 34(6):484–502
- Reddy JN, El-Borgi S (2014) Eringen's nonlocal theories of beams accounting for moderate rotations. *Int J Eng Sci* 82:159–177
- Reddy JN, Srinivasa AR (2014) Non-linear theories of beams and plates accounting for moderate rotations and material length scales. *Int J Non Linear Mech* 66:43–53
- Shahverdi H, Barati MR, Hakimelahi B (2019) Post-buckling analysis of honeycomb core sandwich panels with geometrical imperfection and graphene reinforced nano-composite face sheets. *Mater Res Exp* 6(9):095017
- Shahzad M, Kamran A, Siddiqui MZ, Farhan M (2015) Mechanical characterization and FE modelling of a hyperelastic material. *Mater Res* 18(5):918–924
- She GL, Yuan FG, Ren YR, Liu HB, Xiao WS (2018a) Nonlinear bending and vibration analysis of functionally graded porous tubes via a nonlocal strain gradient theory. *Compos Struct* 203:614–623
- She GL, Ren YR, Xiao WS, Liu HB (2018b) Study on thermal buckling and post-buckling behaviors of FGM tubes resting on elastic foundations. *Struct Eng Mech* 66(6):729–736
- Sheng GG, Wang X (2018) Nonlinear vibration of FG beams subjected to parametric and external excitations. *Eur J Mech A Solids* 71:224–234
- Soares RM, Gonçalves PB (2018) Nonlinear vibrations of a rectangular hyperelastic membrane resting on a nonlinear elastic foundation. *Meccanica* 53(4–5):937–955
- Steinmann P, Hossain M, Possart G (2012) Hyperelastic models for rubber-like materials: consistent tangent operators and suitability for Treloar's data. *Arch Appl Mech* 82(9):1183–1217
- Wang Y, Ding H, Chen LQ (2019) Vibration of axially moving hyperelastic beam with finite deformation. *Appl Math Model* 71:269–285
- Yazid et al (2018) A novel nonlocal refined plate theory for stability response of orthotropic single-layer graphene sheet resting on elastic medium. *Smart Struct Syst* 21(1):15–25
- Younsi et al (2018) Novel quasi-3D and 2D shear deformation theories for bending and free vibration analysis of FGM plates. *Geomech Eng* 14(6):519–532

Publisher's Note Springer Nature remains neutral with regard to jurisdictional claims in published maps and institutional affiliations.